



## ORIGINAL ARTICLE

# A comparative study of microwave and chemically treated *Acacia nilotica* leaf as an eco friendly adsorbent for the removal of rhodamine B dye from aqueous solution



T. Santhi <sup>a,\*</sup>, Ashly Leena Prasad <sup>a</sup>, S. Manonmani <sup>b</sup>

<sup>a</sup> Department of Chemistry, Karpagam University, Coimbatore 641 021, India

<sup>b</sup> Department of Chemistry, PSG College of Arts and Science, Coimbatore 641 014, India

Received 7 October 2010; accepted 20 November 2010

Available online 26 November 2010

## KEYWORDS

*Acacia nilotica*;  
Rhodamine B;  
Adsorption;  
Equilibrium isotherm;  
Kinetics;  
Desorption

**Abstract** The use of cheap and eco friendly adsorbents prepared from freely and abundantly available *Acacia nilotica* leaves have been investigated by batch methods. Microwave treated *A. nilotica* leaves (MVM) are more effective than chemically treated *A. nilotica* leaves (CVM) for the removal of rhodamine B (RH B) from aqueous solution. The effect of initial pH, contact time and initial dye concentration of RH B onto CVM and MVM has been investigated. The applicability of the linear form of Langmuir model to CVM and MVM was proved by the high correlation coefficients  $R^2 = 0.9413$  and  $0.9681$  for RH B adsorption. The  $R^2$  values were greater than 0.994 for all RH B concentrations, which indicates the applicability of the pseudo-second-order kinetic model. The recycling ability of MVM is greater than CVM. The preparation of MVM does not require an additional chemical treatment step and it attains rapid equilibrium. Hence it is agreeing with the principles of green chemistry and less time is required to possess high adsorption of RH B. Therefore, the eco friendly adsorbent MVM is expected to be environmentally and economically feasible for the removal of RH B from aqueous solutions.

© 2010 Production and hosting by Elsevier B.V. on behalf of King Saud University.

\* Corresponding author. Tel.: +91 4222401661; fax: +91 4222611146.

E-mail address: ssnilasri@yahoo.co.in (T. Santhi).

Peer review under responsibility of King Saud University.



Production and hosting by Elsevier

## 1. Introduction

Dyes used in textile industry may be toxic to aquatic organisms and can be resistant to natural biological degradation. Hence, the removal of colour synthetic organic dyestuff from waste effluents becomes environmentally important (Hameed, 2009). The valorization of agricultural wastes into valuable materials without generating pollutants is a big challenge

and is recommended for an industrial sustainable development in order to preserve the environment (Reffas et al., 2010). Adsorption onto activated carbon is proven to be very effective in treating textile wastes. However, in view of the high cost and associated problems of regeneration, there is a constant search for alternate low-cost adsorbents. Such alternatives include coffee ground (Reffas et al., 2010), spent tea leaves (Hameed, 2009), palm ash (Ahmad et al., 2007; Hameed et al., 2007a,b), pomelo (*Citrus grandis*) peel (Hameed et al., 2008), pine-cone (Mahdi et al., 2010), pumpkin seed hull (Hameed and El-Khaiary, 2008), ginger waste (Ahmad and Kumar, 2010), rice husk (Verma and Mishra, 2010).

Rhodamine B, a synthetically prepared carcinogenic xanthine dye is widely used for paper printing, textile dyeing, leather and paint industries. Discharge of RH B into the hydrosphere can cause environmental degradation. In California, rhodamine B is suspected to be carcinogenic and thus products containing it must contain a warning on its label. *Acacia nilotica* is a species of *Acacia*, native to Africa and the Indian subcontinent. In Haryana, *A. nilotica* based agro forestry systems reduced the yield of wheat (Puri et al., 1995).

The aim of the paper is to prepare an eco friendly microwave treated *A. nilotica* leaves as an agricultural waste for the depollution of water effluents contaminated by dyes from textile industry. And to find out the suitability and applicability of carbon prepared by different treatments (microwave and chemical) of *A. nilotica* to uptake cationic dye (rhodamine B) from simulated waste water. The preparation of microwave treated *A. nilotica* leaves was based on green chemistry. Green chemistry is an approach to the design, manufacture and use of chemical products to intentionally reduce or eliminate chemical hazards. The goal of green chemistry is to create better, safer chemicals while choosing the safest, most efficient ways to synthesize them and to reduce wastes. Desorption was used to elucidate the nature of adsorption and recycling of the spent adsorbent.

## 2. Materials and methods

### 2.1. Preparation of chemically treated adsorbent (CVM)

The leaves of *A. nilotica* used in this work were collected locally. It was dried in an oven and treated with conc.  $\text{H}_2\text{SO}_4$  for 12 h and was washed thoroughly with distilled water till it attained neutral pH and was soaked in 2%  $\text{NaHCO}_3$  overnight in order to remove any excess of acid present. Then the material was washed with distilled water and dried.

### 2.2. Preparation of microwave treated eco friendly adsorbent (MVM)

The collected *A. nilotica* leaves were shade-dried and powdered in a grinder. The raw sample is placed in a microwave oven (Samsung; Triple Distribution System) at 800 °C for 2 min. The carbonated sample was preserved in an air tight container for further experiments. No other chemical or physical treatments were used prior to adsorption experiments.

### 2.3. Adsorbate

The commercial grade rhodamine B was used in this work. Rhodamine B (colour index No. 45170) with molecular for-

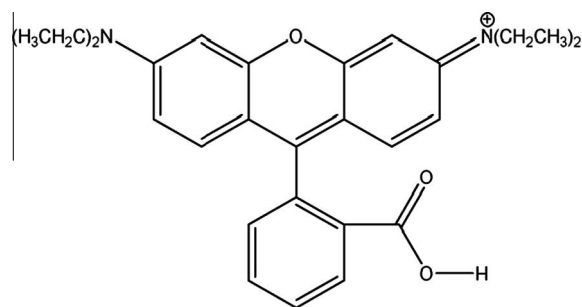


Figure 1 Structure of rhodamine B.

mula  $\text{C}_{28}\text{H}_{31}\text{ClN}_2\text{O}_3$ , molecular weight 479.02 and  $\lambda_{\text{max}}$  554 nm is obtained from Qualigens fine chemicals Mumbai, India. The molecular structure is illustrated in Fig. 1. The dye stock solution ( $500 \text{ mg L}^{-1}$ ) was prepared and the serial dilutions were made by diluting the dye stock solution in accurate proportions to the desired initial concentrations. The initial pH was adjusted with 0.1 M HCl or 0.1 M NaOH. All the chemicals used throughout these studies were of analytical-grade reagents. All the adsorption experiments were carried out at room temperature ( $27 \pm 2 \text{ }^\circ\text{C}$ ).

### 2.4. Characterization of CVM and MVM

The functional groups available on the surface of CVM and MVM were detected using Fourier Transform Infrared (FTIR) analysis. The spectrum was recorded from the range of 4000 to  $500 \text{ cm}^{-1}$ . Determination of zero point charge ( $\text{pH}_{\text{zpc}}$ ) was done to investigate the surface charge of both adsorbents. For the determination of  $\text{pH}_{\text{zpc}}$ , 1 g of the sample suspension was prepared in 50 mL of  $\text{NaNO}_3$  electrolyte of concentration approximately  $10^{-2} \text{ M}$ . Aliquots of suspension were adjusted to various pH values with dil. NaOH and  $\text{HNO}_3$ . After 60 min for equilibrium, the initial pH was measured. Then 0.1 g of  $\text{NaNO}_3$  was added to each aliquot to bring the final electrolyte concentration to about 0.45 M. After an additional 60 min of agitation, final pH was measured. The results were plotted with initial pH (final pH – initial pH) against final pH. The pH at which pH is equal to zero is zero point charge ( $\text{pH}_{\text{zpc}}$ ).

### 2.5. Batch adsorption experiments

The batch adsorption experiments were carried out in order to evaluate the effect of pH, adsorption kinetics, adsorption isotherm and desorption of RH B on CVM and MVM.

#### 2.5.1. Effect of pH on RH B onto CVM and MVM

The effect of pH on the equilibrium uptake of dye was investigated by 50 mL of RH B with initial concentration  $100 \text{ mg L}^{-1}$  was taken in 250 mL shaking flask. The initial pH values adjusted from 2 to 8 were measured using a pH meter (Deluxe pH meter, model-101 E). The initial dye concentration was measured by a double beam UV-vis spectrophotometer (Digital photo colorimeter, model-313) by adjusting the  $\lambda_{\text{max}}$  of the dye. The dye solutions were agitated with about 0.2 g of CVM and MVM in a mechanical shaker at room temperature. Agitation was made for 120 min (RH B onto CVM)

and 90 min (RH B onto MVM) at a constant agitation speed of 160 rpm and the final concentration is measured. The percentage of adsorption was calculated by the following equation:

$$\% \text{ of adsorption} = \frac{\text{COD} - \text{FOD}}{\text{COD}} \times 100 \quad (1)$$

where COD is the controlled optical density and FOD is the final optical density of RH B.

### 2.5.2. Adsorption kinetics

The kinetic experiments were carried out by taking 50 mL of dye solution in 250 mL shaking flasks and treating with 0.2 g of CVM and MVM and were shaken at room temperature. Samples of 1.0 mL were collected from the duplicate flasks at required time intervals viz. 10, 20, 30, 40, 50, 60, 70, 80, 90, 100, 110, 120, 130, 140 and 150 min and were centrifuged for 5 min. The clear solutions were analyzed for residual RH B concentration in the solutions.

### 2.5.3. Adsorption isotherm

Batch adsorption experiments were carried out in a rotary shaker at 160 rpm using 250 mL shaking flasks for 120 min for RH B onto CVM and 90 min for RH B onto MVM. The adsorbents CVM and MVM (0.2, 0.6 and 1 g) were thoroughly mixed with 50 mL of the dye solution. The adsorption isotherms were performed by varying the initial RH B concentrations from 25 to 200 mg L<sup>-1</sup> at pH 7 adjusted before the addition of CVM and MVM. After shaking the flasks for 120 min (RH B onto CVM) and 90 min (RH B onto MVM), the reaction mixtures were analyzed for residual RH B concen-

tration. The amount of dye adsorbed at equilibrium onto carbon,  $q_e$  (mg g<sup>-1</sup>) was calculated by the following mass balance relationship:

$$q_e = (C_o - C_e)V/W \quad (2)$$

where  $C_o$  and  $C_e$  are the initial and equilibrium concentrations (mg L<sup>-1</sup>) of RH B.  $V$  is the volume (L) of the solution and  $W$  is the weight (g) of the adsorbent used.

### 2.5.4. Desorption

Desorption helps to elucidate the nature of adsorption and recycling of the spent adsorbent and the dye. After adsorption experiments the RH B laden carbon was separated out by filtration using Whatman filter paper No. 42 and the filtrate was discarded. The RH B loaded carbon was given a gentle wash with double-distilled water to remove the non-adsorbed RH B if present. The dye loaded samples were agitated with distilled water by adjusting the initial pH from 2 to 7. The desorbed RH B in the solution was separated by centrifugation and analyzed as before. The percentage of desorption was calculated.

## 3. Results and discussion

### 3.1. Characterization of CVM and MVM

The FTIR spectra of CVM and MVM are presented in (Figs. 2a and 2b). The band at 3412 cm<sup>-1</sup> represents the presence of -OH and -NH groups. The bands observed at 2926 and 2856 cm<sup>-1</sup> are associated with asymmetric and symmetric stretching vibrations of -CH group (Ahmad and Kumar,

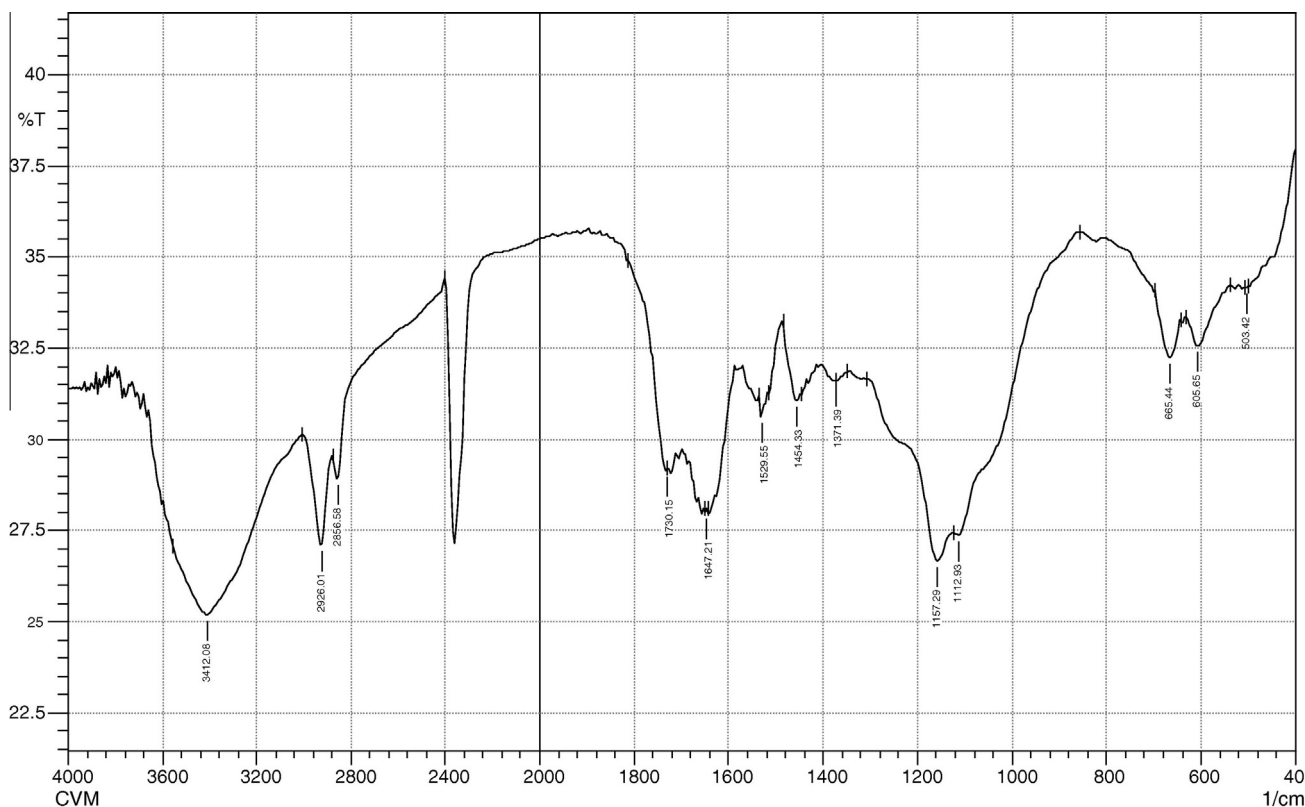


Figure 2a FTIR spectra of CVM.

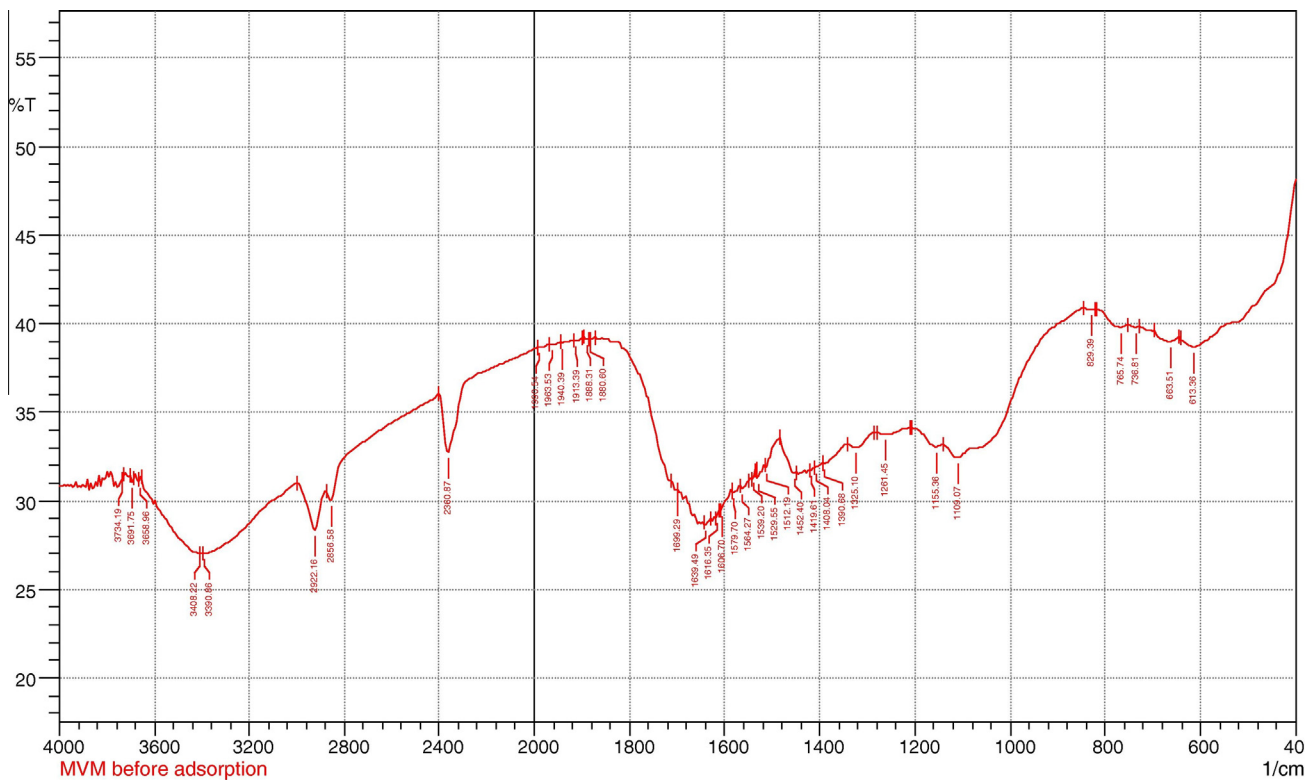


Figure 2b FTIR spectra of MVM.

2010). Atmospheric  $\text{CO}_2$  bands are present at  $2360\text{ cm}^{-1}$  (anti-symmetric  $\text{C}=\text{O}$  stretch) and were observed for MVM only. The bands at  $1637$  and  $1452\text{ cm}^{-1}$  indicate the presence of  $-\text{COO}$ ,  $-\text{C}=\text{O}$  and  $-\text{NH}$  groups for CVM and MVM. The peak at  $1564\text{ cm}^{-1}$  is attributed to the formation of oxygen functional groups such as a highly conjugated  $\text{C}-\text{O}$  stretching in carboxylic groups (Freundlich, 1906) and to the presence of quinone structure (Wang et al., 1998). The bands in the range  $1390\text{--}1406\text{ cm}^{-1}$  which are assigned to  $\text{C}-\text{H}$  bending in alkanes or alkyl groups were observed in MVM (Cengiz and Cavas, 2007). The broad band between  $1325$  and  $1109\text{ cm}^{-1}$  has been assigned to  $\text{C}-\text{O}$  stretching in alcohols and phenols (Freundlich, 1906; Shelden et al., 1993). Another absorption band appearing around  $1261$  and  $663\text{ cm}^{-1}$  can be attributed to the  $\text{Si}-\text{C}$  stretch and  $\text{C}-\text{O}-\text{H}$  twist. The band at  $1261\text{ cm}^{-1}$  implied the  $\text{C}-\text{N}$  stretching of amide similarly present in MVM. The characteristics of CVM and MVM are presented in (Table 1).

Table 1 Physico-chemical characteristics of CVM and MVM.

Parameters	CVM	MVM
Moisture content (%)	21.713	8.713
Ash content (%)	5.95	9.950
pH	6.80	7.020
Decolorizing power ( $\text{mg g}^{-1}$ )	1.100	1.200
Specific gravity	1.240	1.220
Water soluble matter (%)	13.44	12.44
Conductivity ( $\mu\text{s cm}^{-1}$ )	0.210	0.260
Zero point charge ( $\text{pH}_{\text{zpc}}$ )	3.800	4.400
Apparent density ( $\text{g mL}^{-1}$ )	0.256	0.272

### 3.2. Effect of pH on the adsorption of RH B onto CVM and MVM

The effect of initial pH value on the adsorption of RH B onto CVM and MVM was investigated in the range of 2–8. The adsorption capacity increased with increase in solution pH and the maximum adsorption capacity for RH B onto CVM and MVM was observed at pH 7 depicted in Fig. 3. The effect of solution pH is very important when the adsorbing molecules are capable of ionizing in response to the current pH (Hamad et al., 2010). When solution pH increases, high  $\text{OH}^-$  ions accumulate on the adsorbent surface (Ahmad and Kumar, 2010). Therefore, electrostatic interaction between negatively charged adsorbent surface and cationic dye molecule caused the increase in adsorption. Furthermore, the solution pH is above the zero point of charge ( $\text{pH}_{\text{zpc}} = 3.8$  and  $4.4$  for CVM and

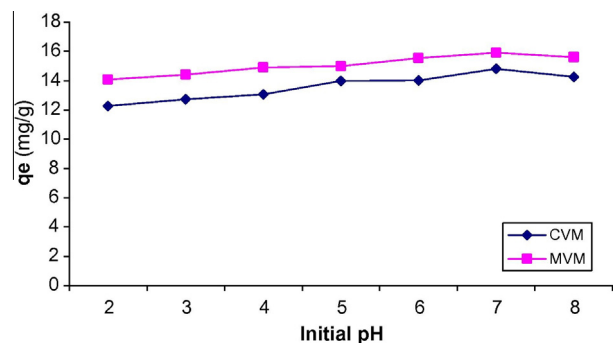


Figure 3 Effect of pH on the adsorption of RH B onto CVM and MVM.

MVM) and hence the negative charged density of the surface of CVM and MVM increased which favors the adsorption of the cationic dye (Janos et al., 2003). The optimum pH value of RH B onto CVM and MVM was 7 and it was used for subsequent experiments.

### 3.3. Effect of contact time and initial concentration on dye adsorption

The uptake of RH B onto CVM and MVM as a function of contact time is shown in Figs. 4a and 4b. It can be seen that the amount of RH B adsorbed per unit mass of adsorbent increased with the increase in initial concentration, although percentage removal decreased with the increase in initial concentration. The uptake of RH B onto CVM and MVM was increased from 5.57 to 20.22 mg g<sup>-1</sup> and 7.13 to 22.13 mg g<sup>-1</sup>, respectively, with the increase in RH B concentration from 50 to 200 mg L<sup>-1</sup>. This may be attributed to an increase in the driving force of the concentration gradient with the increase in the initial dye concentration (Hameed et al., 2008; Ashtoukhy, 2009).

The uptake of RH B onto CVM and MVM was increased with the increase in contact time. The adsorption equilibrium was achieved 110 min for CVM and 90 min for MVM. So compared to MVM, CVM is more time consuming and also the percentage of dye removal is less. Initial adsorption was rapid due to the adsorption of dye onto the exterior surface, after that dye molecules enter into pores (interior surface), a relatively slow process (Ahmad and Kumar, 2010). Data on

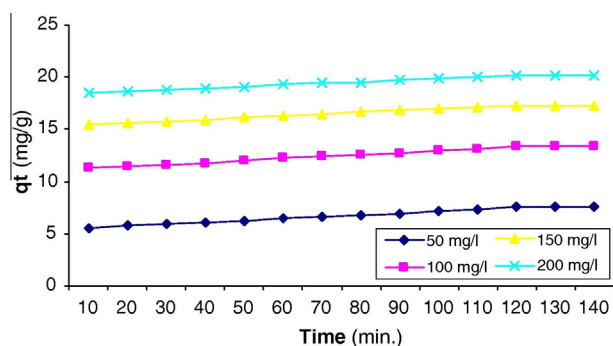


**Figure 4a** Effect of contact time and initial concentration on the adsorption of RH B onto CVM.

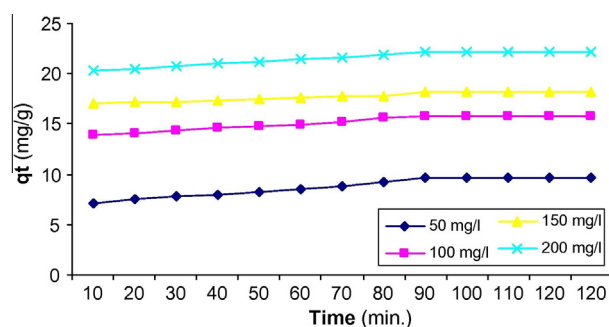


**Figure 4b** Effect of contact time and initial concentration on the adsorption of RH B onto MVM.

the adsorption kinetics of dyes by various adsorbents have shown a wide range of adsorption rates. For example, the effect of contact time on the adsorption of orange-G and crystal violet dye by bagasse fly ash was studied for a period of 24 h for initial dye concentrations of 10 mg L<sup>-1</sup> at 30 °C (Mall et al., 2006). The authors reported that after 4 h of contact, a steady-state approximation was assumed and a quasi-equilibrium situation was accepted (Mall et al., 2006). Dogan et al. (2007) reported that equilibrium time of 180 min was enough for the adsorption of crystal violet and methylene blue dyes by sepiolite for initial dye concentration of 1.2 × 10<sup>-3</sup> mol L<sup>-1</sup> at 30 °C.

### 3.4. Adsorption isotherm

The equilibrium isotherms are used to describe experimental data. The adsorption isotherm is important from both a theoretical and a practical point of view. To optimize the design of an adsorption system for the adsorption of adsorbates, it is important to establish the most appropriate correlation for the equilibrium curves (Altinisik et al., 2010). The equation parameters of these equilibrium models often provide some insight into the sorption mechanism, the surface properties and the affinity of the adsorbent (Bulut et al., 2008). Various isotherm equations like those of Langmuir, Freundlich, Dubinin–Radushkevich (D–R) and Temkin were used to describe the equilibrium characteristics of adsorption.

#### 3.4.1. The Langmuir isotherm

The Langmuir isotherm theory assumes a monolayer coverage of adsorbate over a homogeneous adsorbent surface (Langmuir, 1918). A basic assumption is that sorption takes place at specific homogeneous sites within the adsorbent. Once a dye molecule occupies a site, no further adsorption can take place at that site. The Langmuir adsorption isotherm has been successfully used to explain the adsorption of basic dyes from aqueous solutions (Hameed et al., 2007a,b; Tan et al., 2007). It is commonly expressed as followed:

**Table 2** Isotherm constants for RH B adsorption onto CVM and MVM.

Isotherm model	CVM	MVM
<i>Langmuir</i>		
$Q_m$ (mg g <sup>-1</sup> )	22.371	24.390
$b$ (L mg <sup>-1</sup> )	0.0424	0.0388
$R^2$	0.9413	0.9681
<i>Freundlich</i>		
$1/n$	0.7232	0.4764
$K_f$ (mg g <sup>-1</sup> )	1.9737	2.3232
$R^2$	0.8974	0.9284
<i>Dubinin–Radushkevich</i>		
$Q_m$ (mg g <sup>-1</sup> )	16.2549	16.3691
$K$ (×10 <sup>-5</sup> mol <sup>2</sup> kJ <sup>-2</sup> )	1.000	9.00
$E$ (kJ mol <sup>-1</sup> )	0.2236	0.2357
$R^2$	0.8506	0.8227
<i>Temkin</i>		
$\alpha$ (L g <sup>-1</sup> )	0.3088	0.3929
$\beta$ (mg L <sup>-1</sup> )	5.5566	5.3304
$b$	448.8716	467.5641
$R^2$	0.8997	0.9495

$$q_e = (Q_m K_a C_e) / (1 + K_a C_e) \quad (3)$$

The Langmuir isotherm equation (3) can be linearized into the following form (Kinniburgh, 1986; Longhinotti et al., 1998):

$$C_e/q_e = 1/K_a Q_m + (1/Q_m \times C_e) \quad (4)$$

where  $q_e$  and  $C_e$  are defined before in Eq. (2),  $Q_m$  is a constant and reflect a complete monolayer ( $\text{mg g}^{-1}$ );  $K_a$  is the adsorption equilibrium constant ( $\text{L mg}^{-1}$ ) that is related to the apparent energy of sorption. A plot of  $C_e/q_e$  versus  $C_e$  should indicate a straight line of slope  $1/Q_m$  and an intercept of  $1/(K_a Q_m)$ .

The result obtained from the Langmuir model for the removal of RH B onto CVM and MVM is shown in Table 2 and the theoretical Langmuir isotherm is plotted together with the experimental data points. The correlation coefficients showed strong positive evidence on the adsorption of RH B onto CVM and MVM, which follows the Langmuir isotherm. The applicability of the linear form of Langmuir model to CVM and MVM was proved by the high correlation coefficients  $R^2 = 0.9413$  and  $0.9681$  for RH B adsorption. This suggests that the Langmuir isotherm provides a good model of the sorption system. The maximum monolayer capacity  $Q_m$  obtained from Langmuir is  $22.371$  and  $24.390 \text{ mg g}^{-1}$  for RH B onto CVM and MVM, respectively.

### 3.4.2. The Freundlich isotherm

The Freundlich isotherm (Freundlich, 1906) can be applied to non-ideal adsorption on heterogeneous surfaces as well as multilayer sorption. The Freundlich isotherm can be derived assuming a logarithmic decrease in enthalpy of adsorption with the increase in the fraction of occupied sites and is commonly given by the following non-linear equation:

$$q_e = K_F C_e^{1/n} \quad (5)$$

Eq. (5) can be linearized in the logarithmic form (Eq. (6)) and the Freundlich constants can be determined:

$$\log q_e = \log K_F + \frac{1}{n} \log C_e \quad (6)$$

A plot of  $\log q_e$  versus  $\log C_e$  enables us to determine the constant  $K_F$  and  $1/n$ .  $K_F$  is roughly an indicator of the adsorption capacity related to the bond energy and  $1/n$  is the adsorption intensity of dye onto the adsorbent or surface heterogeneity. The magnitude of the exponent,  $1/n$ , gives an indication of the favorability of adsorption. The value of  $1/n < 1$  represents favorable adsorption condition (Treybal, 1968; Ho and McKay, 1978). The data obtained from linear Freundlich isotherm for the adsorption of the RH B onto CVM and MVM are presented in Table 2. The comparability of the Freundlich model to the Langmuir model was proved by the correlation coefficients  $R^2 = 0.8974$  and  $0.9284$  for adsorption of RH B onto CVM and MVM. The  $1/n$  value is lower than unity, indicating favorable adsorption of RH B onto CVM and MVM.

### 3.4.3. The Dubinin–Radushkevich (D–R) isotherm

The D–R isotherm was also applied to estimate the porosity apparent free energy and the characteristics of adsorption (Dubinin, 1960, 1965; Radushkevich, 1949). It can be used to describe adsorption on both homogenous and heterogeneous surfaces (Shahwan and Erten, 2004). The D–R equation can be defined by the following equation (Dubinin and Radushkevich, 1947; Gregg and Sing, 1982):

$$\ln q_e = \ln Q_m - K \varepsilon^2 \quad (7)$$

where  $K$  is a constant related to the adsorption energy,  $Q_m$  the theoretical saturation capacity,  $\varepsilon$  the Polanyi potential, calculated from Eq. (8):

$$\varepsilon = RT \ln \left( 1 + \frac{1}{C_e} \right) \quad (8)$$

where  $C_e$  is the equilibrium concentration of dye ( $\text{mol L}^{-1}$ ),  $R$  gas constant ( $8.314 \text{ J mol}^{-1} \text{ K}^{-1}$ ) and  $T$  is the temperature (K). By plotting  $\ln q_e$  versus  $\varepsilon^2$ , it is possible to determine the value of  $K$  from the slope and the value of  $Q_m$  ( $\text{mg g}^{-1}$ ) from the intercept, which is  $\ln Q_m$ . The mean free energy  $E$  ( $\text{kJ mol}^{-1}$ ) of sorption can be estimated by using  $K$  values as expressed in the following equation (Hasany and Chaudhary, 1996; Benhammou et al., 2005; Hobson, 1969):

$$E = \frac{1}{\sqrt{2K}} \quad (9)$$

The parameters obtained using above equations were summarized in Table 2. The saturation adsorption capacity  $Q_m$  obtained using D–R isotherm model for adsorption of RH B onto CVM is  $16.2549$  and RH B onto MVM is  $16.3691 \text{ mg g}^{-1}$ . The values calculated using Eq. (9) is  $0.2236$  and  $0.2357 \text{ kJ mol}^{-1}$  for RH B onto CVM and MVM, respectively. This was indicating that physico-sorption played a significant role in the adsorption of RH B onto CVM and MVM.

### 3.4.4. The Temkin isotherm

The Temkin and Pyzhey (Temkin and Pyzhey, 1940) considered the effects of some indirect adsorbate or adsorbate interactions on adsorption isotherms and suggested that because of these interactions the heat of adsorption of all the molecules in the layer would decrease linearly with coverage. The Temkin isotherm has commonly been applied in the following form:

$$q_e = \frac{RT}{b} \ln(AC_e) \quad (10)$$

The Temkin isotherm equation (10) can be simplified to the following equation:

$$q_e = \beta \ln \alpha + \beta \ln C_e \quad (11)$$

where

$$\beta = (RT)/b \quad (12)$$

The constant  $\beta$  is related to the heat of adsorption (Akkaya and Ozer, 2005; Pearce et al., 2003). The adsorption data were analyzed according to the linear form of Temkin isotherm equation (11). The plot of  $\ln C_e$  versus  $q_e$  (Temkin adsorption isotherm) of adsorption of RH B onto CVM and MVM gives the linear isotherm constants and coefficients of determination that are presented in Table 2. The heat of adsorption of RH B onto CVM and MVM was found to be  $4.4887$  and  $4.6756 \text{ kJ mol}^{-1}$ . The correlation coefficients  $R^2$  obtained from Temkin model were comparable to those obtained for Langmuir and Freundlich equations, which explains the applicability of Temkin model to the adsorption of RH B onto CVM and MVM.

It can be seen that the Langmuir isotherm fits the data better than Freundlich, D–R and Temkin isotherms. This high  $R^2$  value indicates that the adsorption of RH B onto CVM and MVM takes place as monolayer adsorption on a surface that

is homogeneous in surface affinity. In this work the adsorption of RH B onto MVM shows better result than the adsorption of RH B onto CVM. Moreover, the MVM does not possess any chemical treatment.

The maximum sorption capacity ( $q_m$ ) of the adsorption of RH B onto CVM and MVM was compared with those reported in literature for different cationic dye adsorption system as shown in Table 3. The performance of the MVM is higher in effectiveness for the removal of cationic dyes.

### 3.5. Adsorption kinetics

The kinetics of adsorbate uptake is important for choosing optimum operating conditions for design purposes. In order to investigate the mechanism of adsorption and potential rate controlling steps such as chemical reaction, diffusion control and mass transport process, kinetic models have been used to test experimental data from the adsorption of RH B onto CVM and MVM. These kinetic models were analyzed using pseudo-first order (Lagergren, 1898), pseudo-second-order (Ho et al., 2000), Elovich and intraparticle diffusion (Weber and Morris, 1963).

#### 3.5.1. Pseudo-first-order equation

The pseudo-first-order equation of Lagergren is generally expressed as follows:

$$\log(q_e - q_t) = \log(q_e) - \frac{K_1}{2.303} t \quad (13)$$

The values of  $q_e$  and  $K_1$  for the pseudo-first-order kinetic model were determined from the intercepts and the slopes of the plots of  $\log(q_e - q_t)$  versus time, respectively (Figs. 5a and 5b). The  $K_1$  values, correlation coefficient values and  $q_e$  values (experimental and calculated) are summarized in Table 4. The correlation coefficient for the pseudo-first-order model changed in the range of 0.913–0.8892 and 0.8921–0.9085 for adsorption of RH B onto CVM and MVM, respectively. Besides, the experimental  $q_e$  values did not agree with the calculated values obtained from the linear plots. It suggests that the kinetics of RH B adsorption onto CVM and MVM did

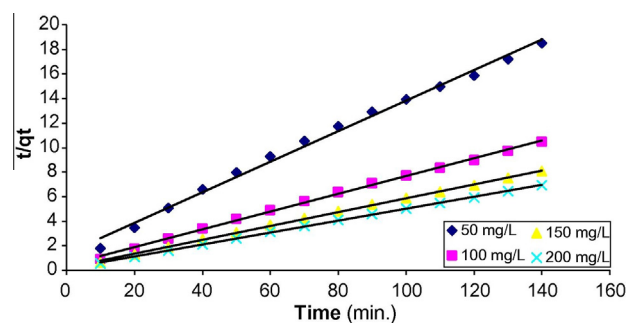


**Figure 5a** Pseudo-second-order kinetics for adsorption of RH B onto CVM at different initial concentrations.

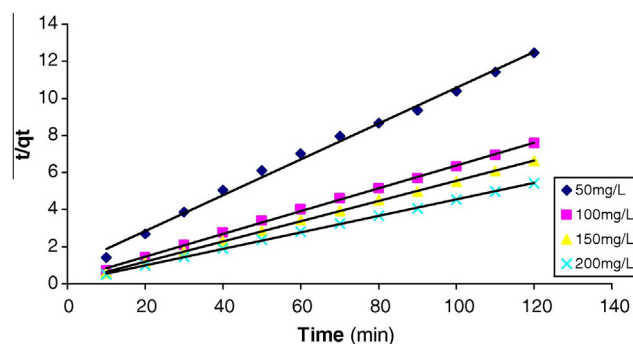


**Figure 5b** Pseudo-second-order kinetics for adsorption of RH B onto MVM at different initial concentrations.

**Table 3** Reported maximum adsorption capacities ( $q_m$  in  $\text{mg g}^{-1}$ ) in the literature for cationic dye obtained on low-cost adsorbents.

Adsorbent	$q_m$ ( $\text{mg g}^{-1}$ )	References
Microwave treated		
<i>Acacia nilotica</i> leaves	24.390	This work
Chemically treated		
<i>Acacia nilotica</i> leaves	22.371	This work
<i>Luffa cylindrical</i>	9.92	Altinisk et al. (2010)
Coffee ground	23.0	Reffas et al. (2010)
activated carbon		
Kolin	5.44	Gupta et al. (2008)
Wheat bran	22.73	Gupta et al. (2007)
Rice bran	14.63	Gupta et al. (2007)
Hen feathers	26.1	Mittal (2006)
Arundo donax root carbon	8.69	Zhang et al. (2008)
Bentonite	7.72	Tahir and Rauf (2006)

**Table 4** First- and second-order kinetic parameters for the adsorption of RH B onto CVM and MVM at different initial concentrations.

Adsorbate	$C_0$ ( $\text{mg L}^{-1}$ )	$q_e(\text{exp})$ ( $\text{mg g}^{-1}$ )	Pseudo-first-order			Pseudo-second-order		
			$K_1$ ( $\text{min}^{-1}$ )	$q_e(\text{cal})$ ( $\text{mg g}^{-1}$ )	$R^2$	$K_2$ ( $\text{g mg}^{-1} \text{min}^{-1}$ )	$q_e(\text{cal})$ ( $\text{mg g}^{-1}$ )	$R^2$
CVM	50	6.54	0.02	3.0768	0.913	0.0112	8.0385	0.994
	100	12.31	0.0209	3.3082	0.877	0.0125	13.7931	0.9981
	150	16.377	0.0225	3.180	0.8833	0.0147	17.6991	0.9992
	200	19.324	0.020	2.7089	0.8892	0.0163	20.5338	0.9995
MVM	50	8.462	0.0234	3.7471	0.8921	0.0102	10.351	0.9946
	100	15.914	0.0253	3.0938	0.8604	0.0160	16.3132	0.9992
	150	17.625	0.0175	1.4167	0.9735	0.0292	18.382	0.9997
	200	21.78	0.0246	2.8497	0.9085	0.0180	22.573	0.9996

not follow the pseudo-first-order kinetic model and hence was not a diffusion-controlled phenomena.

### 3.5.2. Pseudo-second order equation

The pseudo-second order equation is generally given as follows:

$$\frac{t}{q_t} = \frac{1}{K_2 q_e^2} + \frac{1}{q_e} (t) \quad (14)$$

The second-order rate constants were used to calculate the initial sorption rate, given by the following equation:

$$h = K_2 q_e^2 \quad (15)$$

The  $K_2$  and  $q_e$  values determined from the slopes and intercepts of the plot of  $t/q_t$  are presented in Table 4 along with the corresponding correlation coefficients. This is more likely to predict the behavior over the whole range of adsorption. The corresponding correlation coefficients ( $R^2$ ) values for the pseudo-second-order kinetic model were greater than 0.994 for all RH B concentrations, indicating the applicability of the pseudo-second-order kinetic model to describe the adsorption of RH B onto CVM and MVM.

### 3.5.3. Elovich equation

The Elovich equation is another rate equation based on the adsorption capacity generally expressed as the following (Chien and Clayton, 1980; Sparks, 1986; Zeldowitsch, 1934):

$$\frac{dq_t}{dt} = B_E \exp(-A_E q_t) \quad (16)$$

where  $B_E$  is the initial adsorption rate ( $\text{mg g}^{-1} \text{min}^{-1}$ ) and  $A_E$  is the desorption constant ( $\text{g mg}^{-1}$ ) during any experiment.

It is simplified by assuming  $A_E B_E t \gg t$  and by applying the boundary conditions  $q_t = 0$  at  $t = 0$  and  $q_t = q_t$  at  $t = t$  Eq. (16) becomes:

$$q_t = \frac{1}{A_E} \ln(B_E A_E) + \frac{1}{A_E} \ln(t) \quad (17)$$

If RH B adsorption by CVM and MVM fits the Elovich model, a plot of  $q_t$  versus  $\ln(t)$  should yield a linear relationship with a slope of  $(1/A_E)$  and an intercept of  $(1/A_E) \ln(A_E B_E)$  (Figs. 6a and 6b). Thus, the constants can be obtained from the slope and the intercept of the straight line. The initial

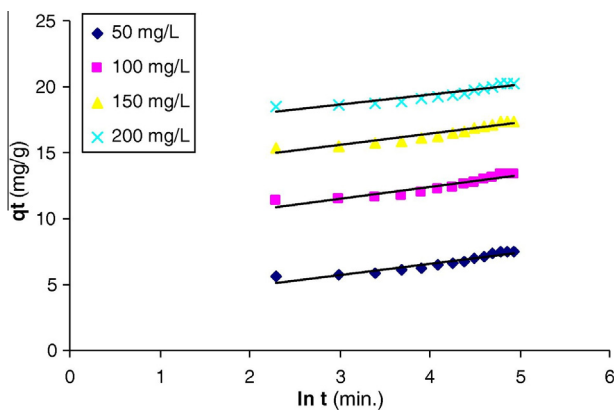


**Figure 6a** Elovich plot for adsorption of RH B onto CVM at different initial concentrations.

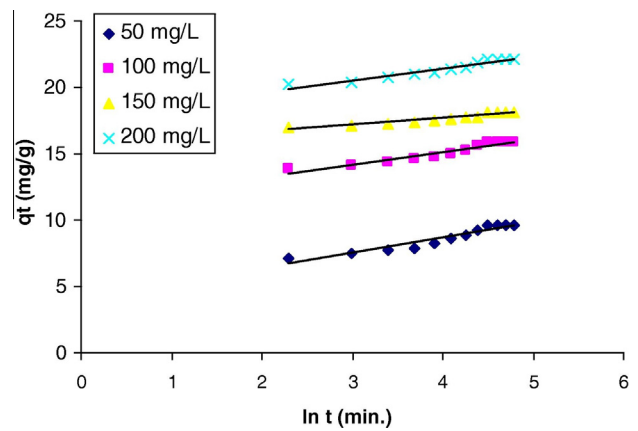


**Figure 6b** Elovich plot for adsorption of RH B onto MVM at different initial concentrations.

adsorption rate  $B_E$  increases from 33.8770 to 18,490,182,279  $\text{mg g}^{-1} \text{min}^{-1}$  for RH B onto CVM and from 35.7244 to 514,378,335  $\text{mg g}^{-1} \text{min}^{-1}$  for RH B onto MVM with the initial RH B concentration from 50 to 200  $\text{mg L}^{-1}$ . Similar pattern is mentioned above for the initial adsorption rate,  $h$ , obtained from pseudo-second-order model. The desorption constant,  $A_E$ , decreases from 1.16225 to 1.3224  $\text{g mg}^{-1}$  for RH B onto CVM and from 1.8552 to 1.1282  $\text{g mg}^{-1}$  for RH B onto MVM with increase and decrease in the initial RH B concentration from 50 to 200  $\text{mg L}^{-1}$ .

### 3.5.4. Intraparticle diffusion

When diffusion (internal surface and pore diffusion) of dye molecule inside the adsorbent is the rate-limiting step, then adsorption data can be presented by the following equation:

$$q_t = K_{\text{dif}} t^{1/2} + C \quad (18)$$

where  $C$  ( $\text{mg g}^{-1}$ ) is the intercept and  $K_{\text{dif}}$  is the intraparticle diffusion rate constant (in  $\text{mg g}^{-1} \text{min}^{-1/2}$ ). The values of  $q_t$  were found to be linearly correlated with values of  $t^{1/2}$  (Figs. 7a and 7b) and the rate constant  $K_{\text{dif}}$  directly evaluated from the slope of the regression line. The values of intercept  $C$  provide information about the thickness of the boundary layer; the resistance to the external mass transfer increases as the intercept increases. The constant  $C$  was found to increase from 4.5529 to 17.575 and 5.8998 to 19.351 with increase in RH B

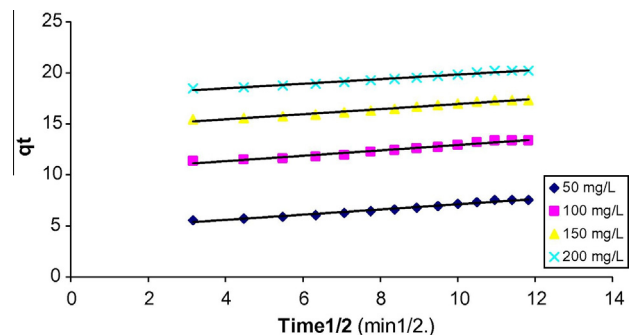


**Figure 7a** Intraparticle diffusion plot for adsorption of RH B onto CVM at different initial dye concentration.

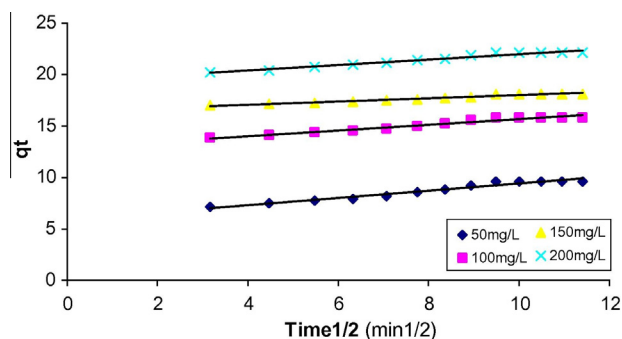


**Figure 7b** Intraparticle diffusion plot for adsorption of RH B onto MVM at different initial dye concentration.

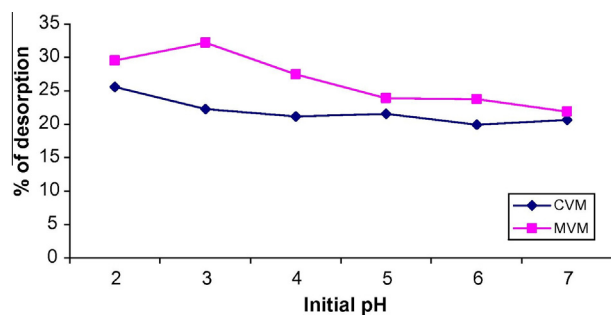


**Figure 8** Desorption of RH B onto CVM and MVM.

concentration from 50 to 200 mg L<sup>-1</sup> onto CVM and MVM, respectively, indicating the increase of the thickness of the boundary layer and decrease of the chance of the external mass transfer and hence increase in the chance of internal mass transfer. The  $R^2$  values are close to unity indicating the application of this model. This may confirm that the intraparticle diffusion is the rate-limiting step. The linearity of the plots demonstrated that intraparticle diffusion played a significant role in the uptake of the RH B onto CVM and MVM. However, as still there is no sufficient indication about it, Ho has shown that if the intraparticle diffusion is the sole rate-limiting step, it is essential for the  $q_t$  versus  $t^{1/2}$  plots to pass through origin (Ho, 2003), which is not the case in Figs. 7a and 7b, it may be concluded that surface adsorption and intraparticle diffusion were concurrently operating during the RH B-CVM and RH B-MVM interactions.

### 3.6. Desorption

Regeneration of the adsorbent may make the treatment more economical and feasible. Desorption helps to elucidate the mechanism of dye adsorption and recycling of the spent adsorbent and the dye. If the adsorbed dyes can be desorbed using neutral pH water, then the attachment of the dye to the adsorbent is by weak bonds (Gad and El-Sayed, 2009). The maximum desorption of RH B onto CVM (25.55) and RH B onto MVM (32.21) is obtained at 2 and 3 pH, respectively (Fig. 8). Desorption of dye by aqueous solutions indicates that the dyes were adsorbed onto the adsorbent through ion-exchange mechanisms.

## 4. Conclusions

From this work, it was found that CVM has a lower adsorption efficiency compared to MVM at any of the given parameters. The equilibrium adsorption is practically achieved in 90 min for RH B onto MVM, but 120 min are taken for the adsorption of RH B onto CVM at 7 pH. The removal efficiency increased with increased agitation time and with initial dye concentrations. The equilibrium data were best described by the Langmuir isotherm model and the adsorption kinetics can be successfully fitted to pseudo-second-order kinetic model with intraparticle diffusion as one of the rate-limiting steps. The recycling ability of MVM is greater than that of CVM. The *A. nilotica* leaves used in this work are freely and abundantly available. The preparation of MVM is agreeing with the principles of green chemistry and less time is required to possess high adsorption of RH B. Therefore, the eco friendly adsorbent MVM is expected to be environmentally and economically feasible for the removal of RH B from aqueous solutions.

## References

- Ahmad, R., Kumar, R., 2010. Adsorption studies of hazardous malachite green onto treated ginger waste. *J. Environ. Manage.* 91, 1032–1038.
- Ahmad, A.A., Hameed, B.H., Aziz, N., 2007. Adsorption of direct dye on palm ash: kinetic and equilibrium modeling. *J. Hazard. Mater.* 141, 70–76.
- Akkaya, G., Ozer, A., 2005. Adsorption of acid red 274 (AR 274) on *Dicranella varia*: determination of equilibrium and kinetic model parameters. *Process. Biochem.* 40, 3559–3568.
- Altinisik, A., Emel, Gur, Yoldas, Seki, 2010. A natural sorbent, *Luffa cylindrical* for the removal of a model basic dye. *J. Hazard. Mater.* 179 (1–3), 658–664.
- Ashtoukhy, E.S.Z.E., 2009. *Loofa egyptiaca* as a novel adsorbent for the removal of direct blue dye from aqueous solution. *J. Environ. Manage.* 90, 2755–2761.
- Benhammou, A., Yaacoubi, A., Nibou, L., Tanouti, B., 2005. Adsorption of metal ions onto Moroccan stevensite: kinetic and isotherm studies. *J. Colloid Interf. Sci.* 282, 320–326.
- Bulut, E., Ozacar, M., Sengil, A.I., 2008. Adsorption of malachite green onto bentonite: equilibrium and kinetic studies and process design. *Micropor. Mesopor. Mater.* 115, 234–246.
- Cengiz, S., Cavas, L., 2007. Removal of methylene blue by invasive marine seaweed: *Caulerpa racemosa* var. *cylindracea*. *Bioresour. Technol.* 99 (7), 2357–2363.
- Chien, S.H., Clayton, W.R., 1980. Application of Elovich equation to the kinetics of phosphate release and sorption on soils. *Soil Sci. Soc. Am. J.* 44, 265–268.
- Dogan, M., Ozdemir, Y., Alkan, M., 2007. Adsorption kinetics and mechanism of cationic methyl violet and methylene blue dyes onto sepiolite. *Dyes Pigments* 75, 701–713.
- Dubinin, M.M., 1960. The potential theory of adsorption of gases and vapors for adsorbents with energetically non-uniform surface. *Chem. Rev.* 60, 235–266.
- Dubinin, M.M., 1965. Modern state of the theory of volume filling of micropore adsorbents during adsorption of gases and steams on carbon adsorbents. *Zh. Fiz. Khim.* 39, 1305–1317.
- Dubinin, M.M., Radushkevich, L.V., 1947. Equation of the characteristics curve of activated charcoal. *Proc. Acad. Sci. USSR* 55, 331–333.
- Freundlich, H., 1906. Uber die adsorption in losungen (Adsorption in solution). *Z. Phys. Chem.* 57, 384–470.

- Gad, H.M.H., El-Sayed, A.A., 2009. Activated carbon from agricultural by-products for the removal of Rhodamine B from aqueous solution. *J. Hazard. Mater.* 168, 1070–1081.
- Gregg, S.J., Sing, K.S.W., 1982. Adsorption, Surface Area and Porosity, second ed. Academic Press, London.
- Gupta, V.K., Ali, I., Saini, V.K., 2007. Adsorption studies on the removal of vertigo blue 49 and orange DNA 13 from aqueous solutions using carbon slurry developed from a waste material. *J. Colloid Interf. Sci.* 315, 87–93.
- Gupta, V.K., Mittal, A., Krishnan, L., Mittal, J., 2008. Adsorption of basic Fuchsin using waste materials – bottom ash and de-oiled soya as adsorbents. *J. Colloid Interf. Sci.* 319, 30–39.
- Hamad, B.K., Ahmad, M.N., Afida, A.R., Asri, M.M.N., 2010. High removal of 4-chloroguaiacol by high surface area oil palm shell-activated carbon activated with NaOH from aqueous solution. *Desalination* 257, 1–7.
- Hameed, B.H., 2009. Spent tea leaves: a non-conventional and low-cost adsorbent for removal of basic dye from aqueous solutions. *J. Hazard. Mater.* 161, 753–759.
- Hameed, B.H., El-Khaiary, M.I., 2008. Removal of basic dye from aqueous medium using a novel agricultural waste material: pumpkin seed hull. *J. Hazard. Mater.* 155, 601–609.
- Hameed, B.H., Ahmad, A.A., Aziz, N., 2007a. Isotherms, kinetics and thermodynamics of acid dye adsorption on activated palm ash. *Chem. Eng. J.* 133, 195–203.
- Hameed, B.H., Ahmad, A.L., Latiff, K.N.A., 2007b. Adsorption of basic dye (methylene blue) onto activated carbon prepared from rattan sawdust. *Dyes Pigments* 75, 143–149.
- Hameed, B.H., Mahmoud, D.K., Ahmad, A.L., 2008. Sorption of basic dye from aqueous solution by pomelo (*Citrus grandis*) peel in a batch system, colloids. *Colloids Surf. A: Physicochem. Eng. Aspects* 316, 78–84.
- Hasany, S.M., Chaudhary, M.H., 1996. Sorption potential of Haro river sand for the removal of antimony from acidic aqueous solution. *Appl. Radiat. Isot.* 47, 467–471.
- Ho, Y.S., 2003. Removal of copper ions from aqueous solution by tree fern. *Water Res.* 37, 2323–2330.
- Ho, Y.S., McKay, G., 1978. Sorption of dye from aqueous solution by peat. *Chem. Eng. J.* 70, 115–124.
- Ho, Y.S., McKay, G., Wase, D.A.J., Foster, C.F., 2000. Study of the sorption of divalent metal ion on to peat. *Adsorp. Sci. Technol.* 18, 639–650.
- Hobson, J.P., 1969. Physical adsorption isotherms extending from ultrahigh vacuum to vapor pressure. *J. Phys. Chem.* 73, 2720–2727.
- Janos, P., Buchtova, H., Ryznarova, M., 2003. Sorption of dye from aqueous solution onto fly ash. *Water Res.* 37, 4938–4944.
- Kinniburgh, D.G., 1986. General purpose adsorption isotherms. *Environ. Sci. Technol.* 20, 895–904.
- Lagergren, S., 1898. On the theory of so called adsorption of dissolved substances. *Handlingar* 24, 1–39.
- Langmuir, I., 1918. The adsorption of gases on plane surface of glass, mica and platinum. *J. Am. Chem. Soc.* 40, 1361–1403.
- Longhinotti, E., Pozza, F., Furlan, L., Sanchez, M.D.N.D., Klug, M., Laranjeira, M.C.M., 1998. Adsorption of anionic dyes on the biopolymer chitin. *J. Braz. Chem. Soc.* 9, 435–440.
- Mahdi, Hadi, Mohammad, R., Samarghandi, R., Gordon, McKay, 2010. Equilibrium two-parameter isotherms of acid dyes sorption by activated carbons: study of residual errors. *Chem. Eng. J.* 160 (2), 408–416.
- Mall, I.D., Srivastava, V.C., Agarwal, N.K., 2006. Removal of orange-G and crystal violet dye by adsorption onto bagasse fly ash-kinetic study and equilibrium isotherm analyses. *Dyes Pigments* 69, 210–223.
- Mittal, A., 2006. Adsorption kinetics of removal of a toxic dye, malachite green, from waste water by using hen feathers. *J. Hazard. Mater.* B133, 196–202.
- Pearce, C.I., Lloyd, J.R., Guthrie, J.T., 2003. The removal of dye from textile waste water using whole bacterial cells: a review. *Dyes Pigments* 58, 179–196.
- Puri, S., Bangarwa, K.S., Singh, S., 1995. Influence of multipurpose trees on agricultural crops in arid regions of Haryana, India. *I. Arid Environ.* 30, 441–451.
- Radushkevich, L.V., 1949. Potential theory of sorption and structure of carbons. *Zh. Fiz. Khim.* 23, 1410–1420.
- Reffas, A., Bernardet, V., David, B., Reinert, L., Bencheikh Lehocine, M., Dubois, M., 2010. Carbon prepared from coffee grounds by H<sub>3</sub>PO<sub>4</sub> activation: characterization and adsorption of methylene blue and nylosan red N-2RBL. *J. Hazard. Mater.* 175, 779–788.
- Shahwan, T., Erten, H.N., 2004. Temperature effects on barium sorption on natural kalinite and chlorite-illite clays. *J. Radioanal. Nucl. Chem.* 260, 43–48.
- Shelden, R.A., Caseri, W.R., Suter, U.W., 1993. Ion exchange on muscovite mica with ultrahigh specific surface area. *J. Colloid Interf. Sci.* 157 (2), 318–327.
- Sparks, D.L., 1986. Kinetics of Reaction in Pure and Mixed Systems in Soil Physical Chemistry. CRC Press, Boca Raton.
- Tahir, S.S., Rauf, N., 2006. Removal of cationic dye from aqueous solution by adsorption onto bentonite clay. *Chemosphere* 63, 1842–1848.
- Tan, I.A.W., Hameed, B.H., Ahmad, A.L., 2007. Equilibrium and kinetic studies on basic dye adsorption by oil palm fibre activated carbon. *Chem. Eng. J.* 127, 111–119.
- Temkin, M.J., Pyzhay, V., 1940. Recent modifications to Langmuir isotherms. *Acta Physicochim. USSR* 12, 217–222.
- Treybal, R.E., 1968. Mass Transfer Operations, second ed. McGraw Hill, New York.
- Verma, V.K., Mishra, A.K., 2010. Kinetic and isotherm modeling of adsorption of dyes onto rice husk carbon. *Global NEST J.* 12 (2), 190–196.
- Wang, J., Huang, C.P., Allen, H.E., Cha, D.K., Kim, D.W., 1998. Adsorption characteristics of dye onto sludge particulates. *J. Colloid Interf. Sci.* 208, 518–528.
- Weber, W.J., Morris, J.C., 1963. Kinetics of adsorption on carbon from solution. *J. Sanit. Eng. Div., Am. Soc. Civil Eng.* 89, 31–59.
- Zeldowitsch, J., 1934. Über den mechanismus der katalytischen oxidation von CO an MnO<sub>2</sub>. *Acta Physicochim. USSR* 1, 364–449.
- Zhang, J., Li, Y., Zhang, C., Jing, Y., 2008. Adsorption of malachite green from aqueous solution onto carbon prepared from *Arundo donax* root. *J. Hazard. Mater.* 150, 774–782.